

Gain-of-Function Mutants of the Cytokinin Receptors AHK2 and AHK3 Regulate Plant Organ Size, Flowering Time and Plant Longevity¹

Isabel Bartrina², Helen Jensen², Ondřej Novák, Miroslav Strnad, Tomáš Werner*, and Thomas Schmuelling*

Institute of Biology/Applied Genetics, Dahlem Centre of Plant Sciences, Freie Universität Berlin, D-14195 Berlin, Germany (I.B., H.J., T.W., T.S.); Laboratory of Growth Regulators, Palacký University, and Institute of Experimental Botany, ASCR, CZ-78371 Olomouc, Slechtitelu 11, Czech Republic (O.N., M.S.); and Institute of Plant Sciences, Department of Plant Physiology, University of Graz, 8010 Graz, Austria (T.W.)

ORCID IDs: 0000-0003-3452-0154 (H.J.); 0000-0002-2806-794X (M.S.); 0000-0001-5179-0581 (T.W.); 0000-0001-5532-9645 (T.S.).

The phytohormone cytokinin is a regulator of numerous processes in plants. In *Arabidopsis* (*Arabidopsis thaliana*), the cytokinin signal is perceived by three membrane-located receptors named ARABIDOPSIS HISTIDINE KINASE2 (AHK2), AHK3, and AHK4/CRE1. How the signal is transmitted across the membrane is an entirely unknown process. The three receptors have been shown to operate mostly in a redundant fashion, and very few specific roles have been attributed to single receptors. Using a forward genetic approach, we isolated constitutively active gain-of-function variants of the *AHK2* and *AHK3* genes, named *repressor of cytokinin deficiency2* (*rock2*) and *rock3*, respectively. It is hypothesized that the structural changes caused by these mutations in the sensory and adjacent transmembrane domains emulate the structural changes caused by cytokinin binding, resulting in domain motion propagating the signal across the membrane. Detailed analysis of lines carrying *rock2* and *rock3* alleles revealed how plants respond to locally enhanced cytokinin signaling. Early flowering time, a prolonged reproductive growth phase, and, thereby, increased seed yield suggest that cytokinin regulates various aspects of reproductive growth. In particular, it counteracts the global proliferative arrest, a correlative inhibition of maternal growth by seeds, an as yet unknown activity of the hormone.

The phytohormone cytokinin regulates numerous developmental processes, including cell proliferation and differentiation, shoot and root growth, seed germination, and leaf senescence (Werner and Schmuelling, 2009; Kieber and Schaller, 2014; Zürcher and Müller, 2016). Cytokinin signaling is mediated by a phosphorelay system that resembles bacterial two-component signaling systems (Hwang and Sheen, 2001; Müller and Sheen, 2007). In *Arabidopsis* (*Arabidopsis thaliana*), there are three membrane-spanning His protein kinases (AHKs) that serve as cytokinin receptors, AHK2, AHK3, and AHK4/CRE1 (named AHK4 in the following; Inoue et al., 2001; Ueguchi et al., 2001; Yamada et al., 2001). The

hormone is recognized and bound by an ~270-amino acid extracytoplasmic binding domain called the CHASE domain (for cyclin His kinase-associated sensory). This domain is flanked by two transmembrane domains and followed toward the C-terminal end on the cytoplasmic side by a His kinase and a receiver domain (Steklov et al., 2013). The three-dimensional structure of the CHASE domain of AHK4 has been resolved by X-ray crystallography (Hothorn et al., 2011). This has revealed that the receptor acts as a dimer and that the hormone is bound by a Per-Arnt-Sim (PAS)-like domain. A simple size-exclusion mechanism allows only for the binding of the free cytokinin bases, which are isopentenyladenine (iP), trans-zeatin (tZ), cis-zeatin (cZ), and dihydrozeatin. Binding of bulkier metabolites such as ribosides and nucleotides is prohibited (Hothorn et al., 2011). This result has been confirmed by an in planta cytokinin receptor-binding assay (Lomin et al., 2015). However, it is clear that the three cytokinin receptors have different affinities for the different cytokinin bases (Suzuki et al., 2001; Spíchal et al., 2004; Romanov et al., 2006; Stolz et al., 2011; Lomin et al., 2015). Interestingly, the ligand affinity of AHK2 resembles that of AHK4, while AHK3 differs from these in its lower affinity to iP (Romanov et al., 2006; Stolz et al., 2011).

The bulk of cytokinin receptors is located in the endoplasmic reticulum (Caesar et al., 2011; Wulfetange et al., 2011; Lomin et al., 2015). Upon ligand binding, the signal is transmitted via an as yet unknown mechanism

¹ This work was supported by the Deutsche Forschungsgemeinschaft (grant no. CRC 429 to T.S. and T.W. and grant no. SPP 1530 to T.S.) and by the Czech Grant Agency (grant no. 15-22322S to M.S.).

² These authors contributed equally to the article.

* Address correspondence to tower@zedat.fu-berlin.de and thomas.schmuelling@fu-berlin.de.

The author responsible for distribution of materials integral to the findings presented in this article in accordance with the policy described in the Instructions for Authors (www.plantphysiol.org) is: Thomas Schmuelling (thomas.schmuelling@fu-berlin.de).

I.B., T.W., and T.S. designed experiments and coordinated the project; I.B. and H.J. performed experiments; O.N. and M.S. carried out hormone analyses; I.B., T.W., and T.S. wrote the article; all authors revised the article.

www.plantphysiol.org/cgi/doi/10.1104/pp.16.01903

across the membrane, the cytoplasmic kinase domain is activated, and the protein autophosphorylates at the His residue. The high-energy phosphoryl group is next transferred within the same molecule to the Asp residue of the receiver domain and from there to His phosphotransfer proteins. These translocate to the nucleus, where they transfer the phosphoryl group to B-type response regulators, which act as transcription factors and orchestrate downstream responses (Müller and Sheen, 2007). In Arabidopsis, the transcript abundance of numerous genes is altered within minutes in response to a cytokinin stimulus (Brenner et al., 2012; Bhargava et al., 2013; Brenner and Schmülling, 2015).

Loss-of-function mutations of single cytokinin receptor genes have no or only weak effects on plant growth, indicating strong functional redundancy (Higuchi et al., 2004; Nishimura et al., 2004; Riefler et al., 2006). Similarly, simultaneous mutation of *AHK2* or *AHK3* together with *AHK4* has only mild effects on development, suggesting that both *AHK2* and *AHK3* alone are sufficient to mediate the central functions of cytokinin. In contrast, *ahk2 ahk3* mutants are dwarfed plants showing stronger root growth, demonstrating the importance of *AHK2* and *AHK3* in regulating vegetative plant growth (Riefler et al., 2006). Additional comprehensive examination of the cytokinin receptor genes also revealed some specialization in cytokinin receptor function (Heyl et al., 2012). For example, it was shown that *AHK4* alone plays a role in embryonic root development, phosphate starvation response, and sulfate assimilation (Mähönen et al., 2000; Maruyama-Nakashita et al., 2004; Franco-Zorrilla et al., 2005). Furthermore, *AHK3* plays a predominant role in regulating leaf senescence and cell differentiation in the transition zone of the root meristem (Kim et al., 2006; Riefler et al., 2006; Dello Ioio et al., 2007). No specific function has been shown for *AHK2* so far.

The functional overlap is particularly high for *AHK2* and *AHK3*, which both contribute to mediate a large number of developmental cytokinin functions, from seed germination to the regulation of shoot growth, and also responses to abiotic stresses, including drought (Tran et al., 2007), cold (Jeon et al., 2010), and high light (Cortleven et al., 2014). The mostly redundant action of *AHK2* and *AHK3* is intriguing and raises the question of why both genes with apparently similar functions have been conserved during evolution. Consistently, *AHK2* and *AHK3* have largely overlapping expression domains, with both being expressed predominantly in shoots (Higuchi et al., 2004). Stolz et al. (2011) showed that both *AHK2* and *AHK3* activate the cytokinin response in leaf mesophyll cells (*AHK4* does not) but that only *AHK3* mediates a response in stomata cells. Interestingly, promoter-swap and domain-swap analyses have shown that *AHK4* can functionally replace *AHK2* but not *AHK3* (Stolz et al., 2011).

In view of the mostly redundant action of the *AHK2* and *AHK3* receptors, it might be informative to study gain-of-function mutants to compare receptor activities. In this work, we report on novel gain-of-function mutants of *AHK2* and *AHK3* named *repressor of cytokinin*

deficiency2 (rock2) and *rock3*, respectively. These mutants were identified in a screen for suppressor mutants of the cytokinin deficiency syndrome displayed by *35S:CKX1*-overexpressing (*CKX1ox*) plants (Niemann et al., 2015). Reversion of the cytokinin deficiency phenotype was due to the constitutive activity of the mutant receptors. The receptor variants do have differential impacts on individual phenotypic traits and, thus, are informative about cytokinin signaling during plant development. These results yield new information on the functions of these evolutionarily closely related receptors and highlight their roles in regulating flowering time and plant longevity. Given the promoting effect of the *rock2* and *rock3* alleles on shoot organ growth and, in particular, seed yield, we propose their potential value for biotechnological approaches.

RESULTS

rock2 and *rock3* Suppress the Cytokinin Deficiency Phenotype

To identify the molecular factors required for establishing the cytokinin deficiency syndrome displayed by *CKX1ox* plants (Werner et al., 2003), we searched for suppressor mutants reverting the dwarf shoot phenotype of *CKX1ox* plants (Niemann et al., 2015). Among others, two mutants named *rock2* and *rock3*, which grew larger than *CKX1ox* (Fig. 1, A and C), were identified and selected for further study. Genetic analysis showed that *rock2* and *rock3* are two dominant second site mutations (Supplemental Table S1). The reversion of the cytokinin-deficient phenotype was already obvious early after germination. In the *CKX1ox* background, *rock2* and *rock3* developed strongly enlarged cotyledons with longer petioles, which even exceeded the size of wild-type cotyledons (Fig. 1B). *rock2 CKX1ox* and *rock3 CKX1ox* plants developed larger rosette leaves, grew taller inflorescence stems with more flowers (Fig. 1, A and C), and the flowers of both suppressor lines were enlarged (Fig. 1D). In addition, both mutations suppressed the late-flowering phenotype of *CKX1ox* plants under long-day conditions (Werner et al., 2003). The rescue was partial in the case of *rock3 CKX1ox*, whereas *rock2 CKX1ox* flowered even earlier than wild-type plants (Fig. 1E). Under short-day conditions, the flowering transition defect of *CKX1ox* plants was more severe as these plants remained in the vegetative stage. Interestingly, only the *rock2* mutation was able to suppress the nonflowering phenotype of *CKX1ox* under short-day conditions (Fig. 1F). In contrast, *rock3 CKX1ox* still failed to flower under short-day conditions. This indicates that *rock2* particularly regulates processes associated with the change from vegetative to reproductive development under different light periods.

Cytokinin is known to delay leaf senescence (Richmond and Lang, 1957; Gan and Amasino, 1995; Riefler et al., 2006), and, consistently, leaves of *CKX1ox* plants showed reduced chlorophyll retention in a detached leaf assay (Fig. 1G). Both *rock2* and *rock3*

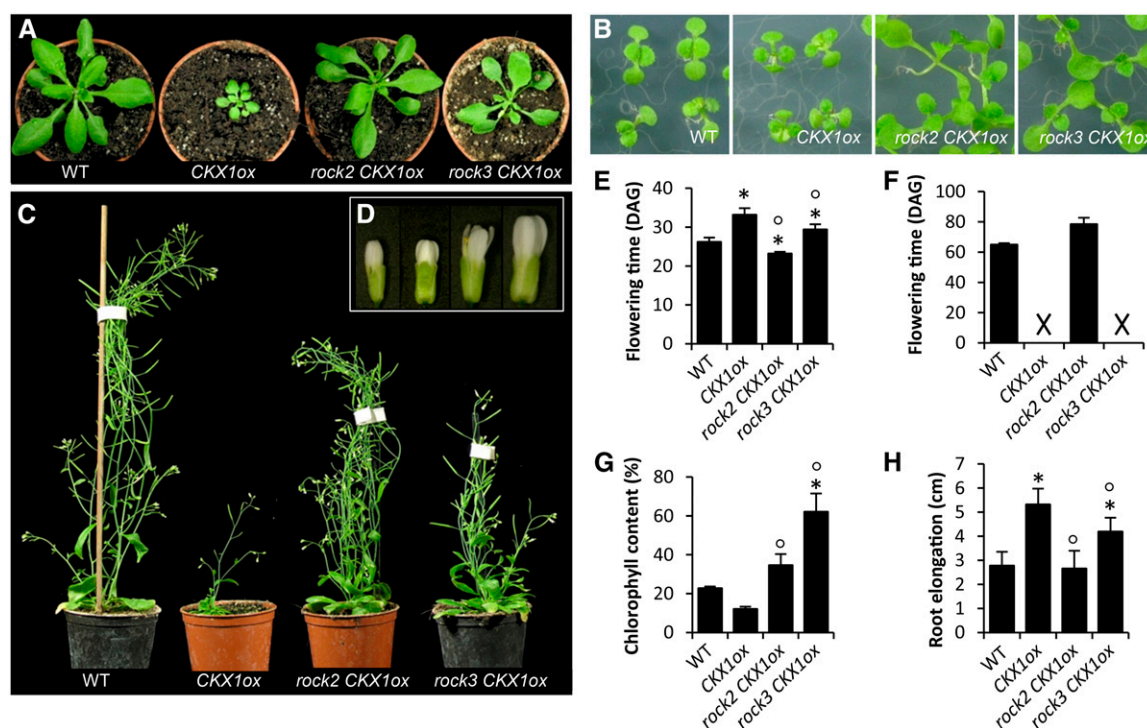


Figure 1. The *rock2* and *rock3* mutations suppress the *CKX1ox* phenotype. A, Morphology of wild-type (WT), *CKX1ox*, *rock2 CKX1ox*, and *rock3 CKX1ox* plants at the rosette stage. Plants were grown for 25 d under long-day conditions. B, *rock2 CKX1ox* and *rock3 CKX1ox* seedlings have larger cotyledons than wild-type and *CKX1ox* seedlings. The photographs were taken 10 d after germination. C, Adult phenotypes of 46-d-old wild-type, *CKX1ox*, *rock2 CKX1ox*, and *rock3 CKX1ox* plants. D, Flowers of wild-type, *CKX1ox*, *rock2 CKX1ox*, and *rock3 CKX1ox* plants (from left to right). E and F, Flowering time of wild-type and mutant plants grown under long-day (E) or short-day (F) conditions. Crosses indicate that no transition to flowering occurred ($n = 20$). DAG, Days after germination. G, Relative leaf chlorophyll content of the fourth and fifth leaves of 3-week-old soil-grown plants after 7 d in the dark. Chlorophyll content before the start of dark incubation was set to 100% ($n = 3$). H, Root elongation of seedlings between day 3 and day 9 after germination ($n \geq 25$). Error bars represent sd. The statistical significance of differences was calculated by two-way ANOVA. *, $P < 0.01$ compared with the wild type; °, $P < 0.05$ compared with *CKX1ox* plants.

retarded the breakdown of chlorophyll of *CKX1ox* plants during dark-induced senescence compared with wild-type and *CKX1ox* plants. After 7 d in the dark, the leaf chlorophyll content was reduced by almost 80% in the wild type and by 90% in *CKX1ox* plants, while it was decreased only by 65% and 35% in *rock2 CKX1ox* and *rock3 CKX1ox* mutants, respectively. This indicates that *rock3* plays a more prevalent role than *rock2* in delaying dark-induced leaf senescence.

To study whether *rock2* and *rock3* also eventually exert a differential influence on root development, we compared primary root elongation in the mutants and the wild type. Figure 1H shows that the roots of *rock2 CKX1ox* seedlings displayed a complete reversion, and those of *rock3 CKX1ox* seedlings showed a partial reversion, of the enhanced primary root elongation caused by the reduced cytokinin content of *CKX1ox* seedlings (Werner et al., 2003).

rock2 and *rock3* Increase Sensitivity toward Exogenous Cytokinin

What could be the cause for the suppression of the cytokinin deficiency phenotype of *CKX1ox* plants?

Analysis of the expression of the *CKX1* transgene in both the *rock2* and *rock3* mutants showed that it was not affected by the mutation (Fig. 2A). In addition, outcrossing the *35S:CKX1* transgene from the *rock2 CKX1ox* or *rock3 CKX1ox* background revealed that the transgene was functionally intact (data not shown). Comparison of the cytokinin content of wild type, *CKX1ox*, *rock2*, and *rock3* seedlings showed that the mutations did not increase the endogenous cytokinin content compared with *CKX1ox* (Fig. 2B; Supplemental Table S2). This suggested that a mechanism different from interference with *35S:CKX1* gene expression or metabolic compensation must be the cause of the phenotypic reversion.

Next, we analyzed whether *rock2* and *rock3* change the plants' sensitivity to exogenously applied cytokinin. Figure 2C shows that wild-type seedlings grew smaller on medium containing 25 nM BA; however, with the exception of a few yellowing leaves, most leaves stayed green. *CKX1ox* seedlings were less sensitive and grew on BA-containing medium similar as on medium without BA. In contrast, *rock2 CKX1ox* and *rock3 CKX1ox* seedlings showed strong hypersensitive reactions to cytokinin. They stayed smaller than control

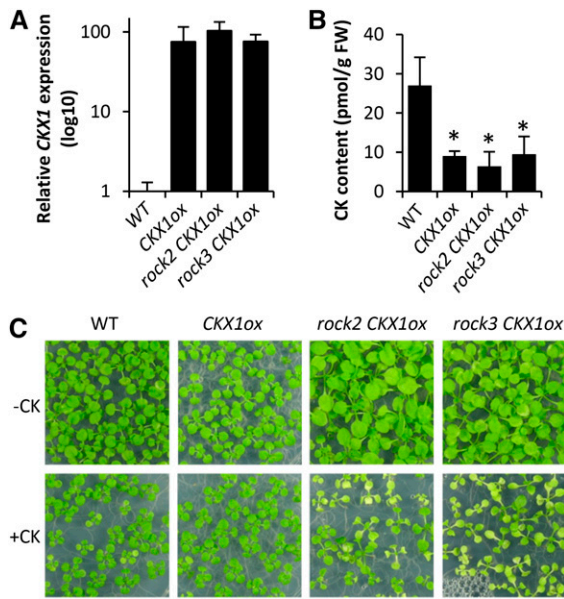


Figure 2. *rock2* and *rock3* mutations alter cytokinin sensitivity. A, Real-time quantitative (q)PCR analysis of *CKX1* transcript levels in seedlings grown in vitro for 10 d. Expression values were normalized to *PP2AA2*, and expression in the wild type (WT) was set to 1. Values are averages of three biological replicates \pm SE. B, Total cytokinin (CK) contents of 2-week-old seedlings. Contents of individual cytokinin metabolites are shown in Supplemental Table S1. Error bars represent SD. *, $P < 0.05$ compared with the wild type as calculated by two-way ANOVA. FW, Fresh weight. C, Phenotypes of 14-d-old seedlings grown on medium without (–CK) or with 25 nM benzyladenine (BA; +CK). *rock2 CKX1ox* and *rock3 CKX1ox* develop pale yellow leaves and show reduced shoot growth.

plants grown on standard medium and formed yellow leaves, which is a typical reaction to high exogenous cytokinin concentrations (Ainley et al., 1993). The altered growth responses indicate that *rock2* and *rock3* enhance the plants' cytokinin sensitivity and suggest that the altered sensitivity may be causal for the suppression of the cytokinin-deficient phenotype.

rock2 and *rock3* Encode Novel Dominant Gain-of-Function Alleles of *AHK2* and *AHK3*

Intriguingly, genetic mapping of the *rock2* and *rock3* mutations revealed that both were located in genes coding for different cytokinin receptors. The *rock2* mutation turned out to be a C-to-T transition in the seventh exon of the *AHK2* (*At5g35750*) gene, leading to a semi-conservative substitution of aliphatic Leu by aromatic Phe at amino acid position 552 (L552F) in the fourth predicted transmembrane domain (Fig. 3, A and B). The *rock3* mutation was identified as a single base change from C to T in the second exon of *AHK3* (*At1g27320*). This results in a nonconservative amino acid change from polar Thr to aliphatic Ile at position 179 (T179I) located close to the predicted cytokinin-binding domain of the *AHK3* receptor (Fig. 3, A and B). A second

independent allele, named *rock3-2*, was identified during the course of this work and caused the exchange of negatively charged Glu to positively charged Lys at position 182 (E182K) in close proximity to the T179I mutation (Fig. 3A). The first identified allele *rock3-1* was used for all analyses described in this article and is called *rock3* throughout.

To prove that the identified mutant alleles of *AHK2* and *AHK3* are causal for the suppression of the cytokinin-deficient phenotype, the mutant gene variants were cloned under the control of their native promoters and transformed in the *CKX1ox* background. Transforming *CKX1ox* was inherently difficult; nevertheless, two independent transgenic *AHK2:rock2 CKX1ox* lines and three independent *AHK3:rock3 CKX1ox* lines

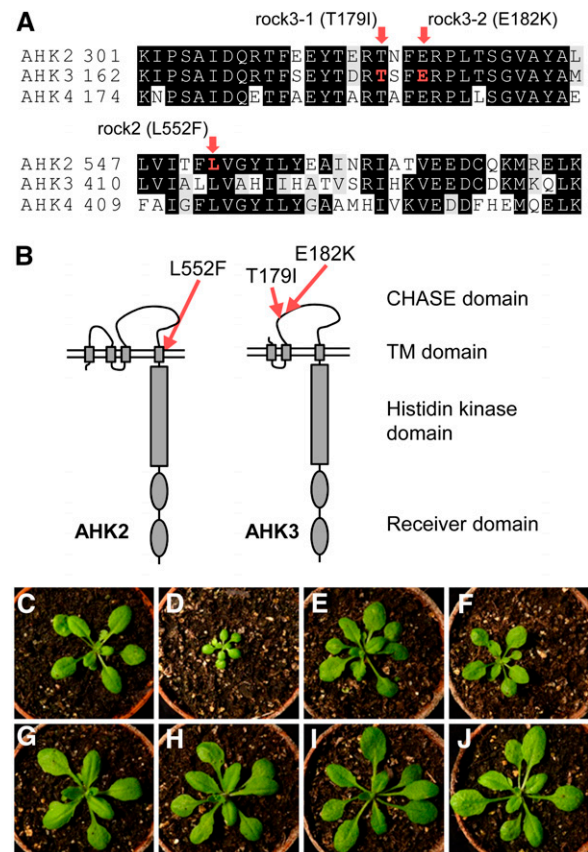


Figure 3. *rock2* and *rock3* are novel gain-of-function alleles of the *AHK2* and *AHK3* genes. A, Two segments of the sequence alignment between the cytokinin receptor proteins *AHK2*, *AHK3*, and *AHK4*. The amino acid residues that are mutated (shown in red) in *rock2* and *rock3* are conserved in all three receptors. Full-length *AHK* protein sequences were aligned using ClustalW. B, Schematic representation of the *AHK2* and *AHK3* protein domains and the positions of amino acid substitutions (red arrows) corresponding to the *rock2* and *rock3* mutations. TM, Transmembrane. C to J, Genetic complementation of the *CKX1ox* phenotype by *AHK2:rock2* and *AHK3:rock3*. Two independent transgenic *AHK2:rock2* (G and H) and *AHK3:rock3* (I and J) lines in the *CKX1ox* background are shown in comparison with the wild type (C), *CKX1ox* (D), *rock2 CKX1ox* (E), and *rock3 CKX1ox* (F) at 18 d after germination.

were identified. All five transgenic lines showed a suppression of the cytokinin deficiency phenotype similar to or even stronger than the *rock2 CKX1ox* and *rock3 CKX1ox* suppressor lines (Fig. 3, C–J). This unequivocally confirmed that the phenotypes were caused by the mutations in the *AHK2* and *AHK3* genes. Thus, *rock2* and *rock3* encode two novel dominant gain-of-function variants of the cytokinin receptors AHK2 and AHK3.

rock2 and *rock3* Enhance Cytokinin Signaling

The revertant morphology and the enhanced cytokinin sensitivity indicated that the *rock2* and *rock3* alleles might code for cytokinin receptors with increased signaling activity. To test whether the mutant receptors act in a cytokinin-independent manner or could be activated by lower cytokinin concentrations, we used the yeast (*Saccharomyces cerevisiae*) complementation assay described by Inoue et al. (2001). In this assay, *AHK4* rescues, in a cytokinin-dependent manner, the survival of a yeast mutant that lacks the endogenous His kinase *SLN1* (Inoue et al., 2001). It is known that the yeast Δ *sln1* strain carrying one of the other two cytokinin receptors (*AHK2* or *AHK3*) can grow in the absence of cytokinin, but growth may be accelerated in the presence of cytokinin (Mähönen et al., 2006; Tran et al., 2007). However, under our laboratory conditions, the cytokinin-dependent faster growth rate of strains containing *AHK2* or *AHK3* receptor genes was not observed; therefore, we were not able to test the original *rock2* or *rock3* mutation in this system. Instead, we constructed *rock2* and *rock3* variants of *AHK4* (named *AHK4^{rock2}* and *AHK4^{rock3}*), as the positions affected by the *rock2* and *rock3* mutations are conserved in all three cytokinin receptors of Arabidopsis (Fig. 3A). Both *rock* variants of *AHK4* suppressed the lethality of the Δ *sln1* mutation even without the addition of cytokinin to the medium, while the mutant carrying the wild-type *AHK4* allele showed strictly cytokinin-dependent growth rescue (Fig. 4A). This shows that the His kinase activity of *AHK4^{rock2}* and *AHK4^{rock3}* is independent of cytokinin and that *rock2* and *rock3* may be constitutively active receptor proteins.

To test further the effects of *rock2* and *rock3* on cytokinin signaling output in planta, we compared the expression level of the well-established cytokinin reporter *ARR5* in the wild type and both *rock* mutants. Figure 4B shows increased steady-state mRNA levels of *ARR5* in *rock2* and *rock3*, indicating enhanced cytokinin signaling in planta. Next, we introgressed the mutant alleles (without the *35S:CKX1* transgene) into a line harboring the *ARR5:GUS* reporter (D'Agostino et al., 2000). Figure 4, B to J, shows strongly increased GUS activity in all analyzed tissues of *rock2* *ARR5:GUS* and *rock3* *ARR5:GUS* seedlings. Seven days after germination increased, GUS activity was detected in the vascular tissue of cotyledons and leaves, the shoot apex, the root vasculature, the vascular procambium, and the root cap of the primary roots. *rock2* caused an overall stronger increase

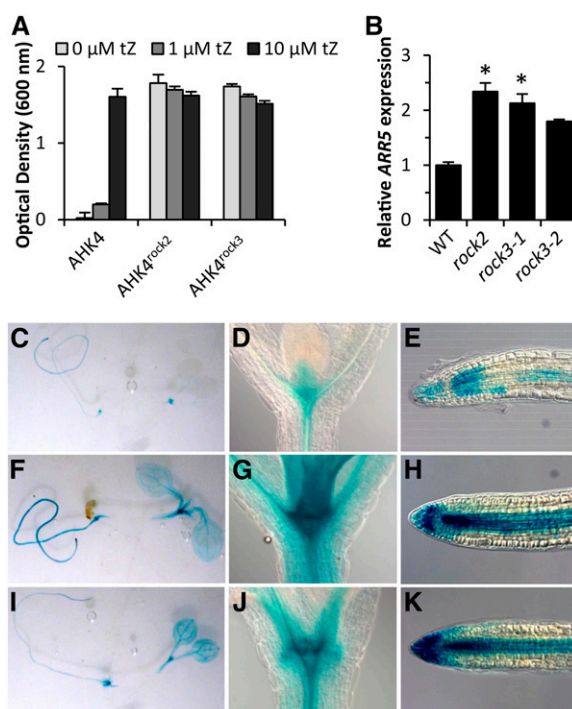


Figure 4. The *rock2* and *rock3* genes code for constitutively active receptors. A, Suppression of the lethal *sln1Δ mutation by His kinase activity of *AHK4^{rock2}* and *AHK4^{rock3}*. The growth of the *sln1Δ yeast strain expressing *AHK4^{rock2}* or *AHK4^{rock3}* was independent of the presence of cytokinin. Error bars represent sd ($n = 3$). B, Relative expression levels of *ARR5* in the *rock* mutants compared with wild type (WT). qPCR analysis was performed using 5-d-old seedlings grown in vitro. Values are averages of three biological replicates \pm SE. The statistical significance of differences compared with the wild type was calculated by ANOVA. *, $P < 0.01$. C to K, Histochemical analysis of *ARR5:GUS* activity in the wild-type (C–E), *rock2* (F–H), and *rock3* (I–K) backgrounds. Images show whole seedlings and shoot apices of 5-d-old plants stained overnight and primary root tips of 7-d-old plants after 30 min of staining (from left to right).**

in GUS activity than *rock3* in all analyzed tissues. For example, *rock2* mutants showed high GUS activity along the whole root, whereas in *rock3* roots, the GUS signal was increased only weakly in the apical part of the root. This correlates well with the observed stronger capacity of *rock2* to suppress the cytokinin deficiency phenotypes in shoot and root. The enhanced expression of the cytokinin response gene *ARR5:GUS* as an output of the cytokinin signaling system, together with the results of the yeast complementation assay, show that the constitutively active *rock2* and *rock3* activate more strongly the cytokinin signal transduction pathway.

Previous work has provided indications that cytokinin signaling is intimately linked to the metabolic homeostasis of the hormone (Riefler et al., 2006). The identified more active receptors provide an opportunity to test this link further. Therefore, we analyzed whether the endogenous cytokinin concentration responds to the enhanced cytokinin signaling and determined the cytokinin levels of wild-type, *rock2*, and *rock3* seedlings and seedlings expressing *AHK2:rock2*.

Both *rock* mutants and the transgenic line showed similar reductions of 45% to 56% of the total cytokinin content (Table I). Stronger differences between *rock2* and *rock3* were found for the biologically active free bases. Both the *rock2* mutation and transgenic expression of *AHK2:rock2* caused a decrease of about 40% for iP and cZ and of about 55% for tZ in comparison with the wild type (Table I). In *rock3* seedlings, the levels of iP, tZ, and cZ were reduced only by 24%, 11%, and 14%, respectively, in comparison with wild-type seedlings. Taken together, the gain-of-function alleles of *AHK2* and *AHK3* have an impact on cytokinin homeostasis and lower the cytokinin content, supporting a feedback regulation of cytokinin metabolism by the cytokinin signaling pathway. Moreover, these results corroborate the hypothesis that these receptor variants display a high signaling activity independent of the steady-state cytokinin concentration.

rock2 and *rock3* Increase Shoot Growth and Leaf Size

The functional redundancy within the cytokinin receptor family makes it difficult to dissect the biological functions of individual receptor proteins. In this situation, gain-of-function receptor variants can be useful to obtain information on their individual functions. Therefore, we analyzed the consequences of the *rock2* and *rock3* mutations on growth and development in more detail using lines containing the original *rock* mutations in the wild-type background as well as transgenic lines expressing the *rock2* and *rock3* coding sequences under the control of their native promoters. Results are shown for homozygous progeny of lines *AHK2:rock2-10* and *AHK3:rock3-1*. Two other independent lines, *AHK2:rock2-7* and *AHK3:rock3-5*, showed similar results. qRT-PCR analysis showed that the levels of *AHK2* transcripts were similar in the wild type, *rock2*, and the transgenic *AHK2:rock2* line (Supplemental Fig. S1A). Likewise, the wild type, *rock3*, and the transgenic *AHK3:rock3* line had comparable *AHK3* transcript levels (Supplemental Fig. S1B).

Figure 5 shows different aspects of the shoot development in these plants. *rock2* mutants and transgenic plants grew significantly taller than wild-type plants (Fig. 5, A and B). The inflorescence stems of 50-d-old wild-type and *rock3* mutant plants measured 33.2 ± 1.3 cm and 35.4 ± 2.3 cm in height (7% increase). *rock2* mutant plants grew 42%, transgenic *AHK3:rock3* plants grew 60%, and transgenic *AHK2:rock2* plants grew even 85% taller than wild-type plants. All the mutant and transgenic lines also had increased stem diameter (Fig. 5, C–E). Also, in this case, the transgenic lines showed the strongest increase, and the stem diameter was increased up to about 36% in comparison with the wild type. Transverse sections of the primary inflorescence stem showed that stem morphology was normal in all genotypes, but the number of cells in stems of transgenic lines was higher than in wild-type stems. Figure 5E shows as an example of transverse sections of wild-type and *AHK3:rock3* inflorescence stems. The increased cell number could be due to a higher cambial activity, which has been shown previously to be regulated by cytokinin (Matsumoto-Kitano et al., 2008; Nieminen et al., 2008; Bartrina et al., 2011). This, however, will require further clarification.

Further inspection of the shoot phenotype revealed that *rock2* and *rock3* also positively regulate shoot lateral organ size. *rock2* and *rock3* seedlings developed strongly enlarged cotyledons (Fig. 6A), a phenotype that was more prominent in transgenic *rock2* and *rock3* lines. Later during development, *rock2* and *rock3* mutants formed larger rosette leaves (Fig. 6B), with the *AHK2:rock2* and *AHK3:rock3* transgenic lines forming the largest leaves. The biomass of rosette leaves was increased in *rock2* and *rock3* mutants (Fig. 6C). As organ size is influenced by cell number and cell expansion, we analyzed the size of epidermal cells in the sixth fully developed rosette leaf of wild-type and *rock2* plants. The epidermal cell size of *rock2* plants was slightly but not significantly reduced (Fig. 6D). This, together with the increased leaf surface (Fig. 6E), revealed that *rock2* rosette leaves formed about 40% to 50% more epidermal cells compared with the wild type. In conclusion,

Table I. Cytokinin content of *rock2* and *rock3*

Genotype	iP	iPR	iPRMP	iP9G	tZ	tZR	tZRMP	Z9G
Wild type	1.91 ± 0.33	1.28 ± 0.18	2.18 ± 0.55	1.38 ± 0.09	0.71 ± 0.17	0.67 ± 0.19	1.29 ± 0.38	5.74 ± 0.90
<i>rock2</i>	1.13 ± 0.26	1.01 ± 0.18	2.23 ± 0.03	0.72 ± 0.06	0.32 ± 0.04	0.24 ± 0.05	0.40 ± 0.12	1.56 ± 0.38
<i>AHK2:rock2</i>	1.06 ± 0.29	1.25 ± 0.21	1.99 ± 0.31	0.93 ± 0.11	0.31 ± 0.01	0.23 ± 0.02	0.44 ± 0.09	1.88 ± 0.48
<i>rock3</i>	1.45 ± 0.41	1.08 ± 0.21	1.31 ± 0.07	0.84 ± 0.10	0.63 ± 0.11	0.20 ± 0.02	0.23 ± 0.06	1.30 ± 0.10
Genotype	tZOG	tZROG	cZ	cZR	cZRMP	cZOG	cZROG	
Wild type	5.66 ± 1.00	0.46 ± 0.10	0.23 ± 0.04	0.89 ± 0.20	4.40 ± 0.76	12.26 ± 1.82	3.95 ± 1.27	
<i>rock2</i>	1.83 ± 0.36	0.20 ± 0.03	0.14 ± 0.02	0.75 ± 0.23	3.15 ± 0.12	3.65 ± 0.18	4.46 ± 0.13	
<i>AHK2:rock2</i>	1.67 ± 0.35	0.26 ± 0.03	0.13 ± 0.01	0.93 ± 0.18	3.84 ± 0.73	6.11 ± 1.78	4.33 ± 0.81	
<i>rock3</i>	0.98 ± 0.04	0.21 ± 0.01	0.20 ± 0.05	1.02 ± 0.20	3.63 ± 1.03	3.92 ± 0.82	3.13 ± 0.45	

Arabidopsis seedlings (14 d after germination) were analyzed. iPR, N^6 -(Δ^2 -isopentenyl)adenosine; iPRMP, N^6 -(Δ^2 -isopentenyl)adenosine 5'-monophosphate; iP9G, N^6 -(Δ^2 -isopentenyl)adenine 9-glucoside; tZR, trans-zeatin riboside; tZRMP, trans-zeatin riboside 5'-monophosphate; tZ9G, trans-zeatin 9-glucoside; tZOG, trans-zeatin O-glucoside; tZROG, trans-zeatin riboside O-glucoside; cZR, cis-zeatin riboside; cZRMP, cis-zeatin riboside 5'-monophosphate; cZOG, cis-zeatin O-glucoside; cZROG, cis-zeatin riboside O-glucoside. Data shown are pmol g⁻¹ fresh weight ± SD; n = 3.

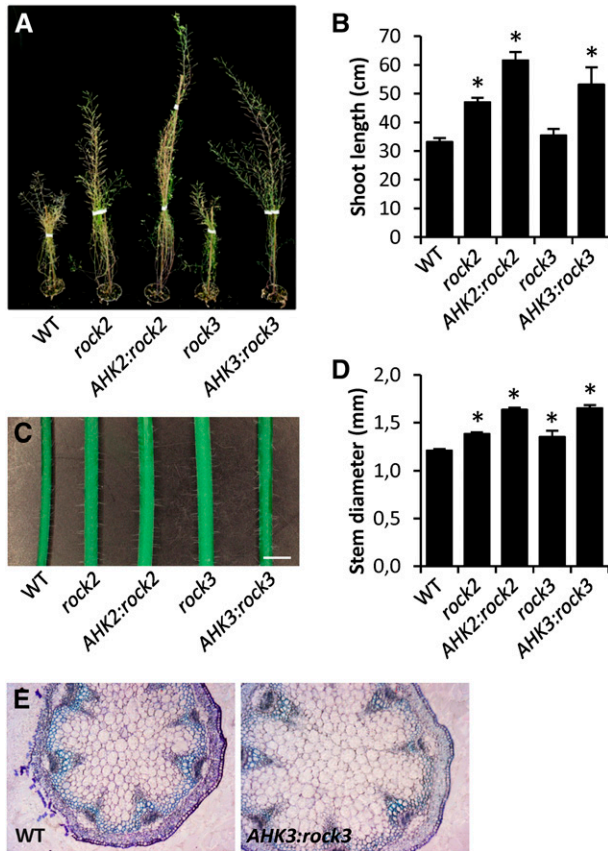


Figure 5. Enhanced shoot growth of *rock2* and *rock3* mutants and transgenic plants. A and B, Height of the main inflorescence stem after the termination of flowering (50 d after germination). C and D, Primary inflorescence stems 3 cm above the rosette (C) and their diameter (D). Bar in C = 2 mm. The statistical significance of differences in B and D compared with the wild type (WT) was calculated by ANOVA. *, $P < 0.001$. Error bars represent sd. E, Stem sections of wild-type and *AHK3:rock3* plants at the base of primary inflorescence stems. Sections were stained with Toluidine Blue.

the *rock2*-dependent changes in organ size are due to prolonged mitotic activity and/or faster cell proliferation during leaf growth.

rock3 Prolongs the Life Span of Leaves

It is known that cytokinin delays leaf senescence (Gan and Amasino, 1995; Kim et al., 2006). We compared the natural senescence as well as the dark-induced senescence of detached leaves of *rock2* and *rock3* with that of the wild type. Visual examination of the sixth rosette leaves throughout their life spans showed that the onset of natural leaf senescence was delayed particularly in *rock3* mutant plants (Fig. 7A). *rock3* leaves had an ~7-d-longer life span compared with wild-type leaves, whereas *rock2* leaves showed only a slightly delayed leaf senescence, up to 2 d (Fig. 7A). These results were confirmed by measuring the photosynthetic efficiency of PSII (F_v/F_m), which was maintained about 4 d longer at a high level in

leaves of *rock2* and about 8 d longer in *rock3* plants (Fig. 7B). Figure 7C shows that dark-induced leaf senescence also was strongly retarded in *rock3* mutant plants. After 7 d in the dark, the chlorophyll content was reduced to 10% in wild-type and *rock2* plants, whereas *rock3* leaves were still green, with a remaining chlorophyll content of almost 60%. These results show that a gain-of-function mutation in the AHK3 cytokinin receptor significantly delays different senescence-associated symptoms in Arabidopsis. Enhanced activity of AHK2, on the other hand, has only a minor but still significant impact on delaying leaf senescence.

The strong delay of leaf senescence in *rock3* mutants prompted us to compare *rock3* with another AHK3 allele, *ore12*, reported to delay leaf senescence (Kim et al., 2006). Both the visual inspection and the F_v/F_m values showed significantly later onset of senescence in *rock3* than in *ore12* (Supplemental Fig. S2), indicating quantitatively different effects of these mutations on AHK3 receptor activity.

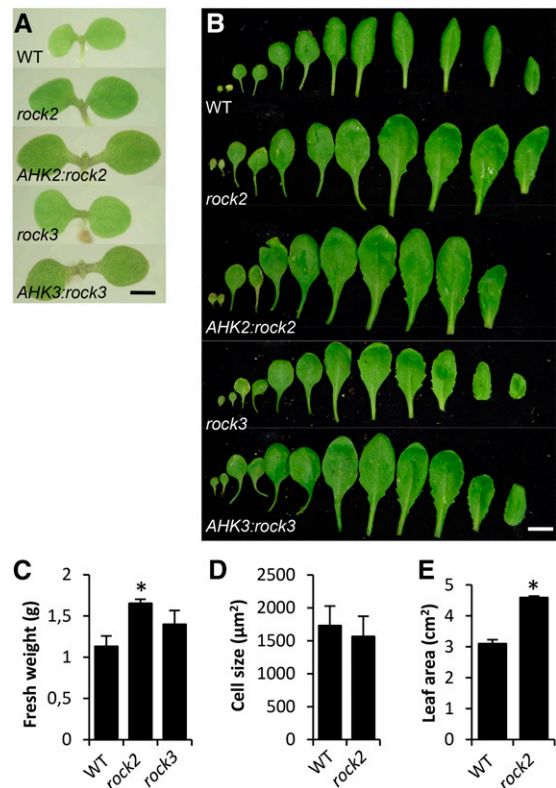


Figure 6. Leaf phenotypes of *rock2* and *rock3* mutants and transgenic plants. A, Cotyledon size of 5-d-old seedlings. Bar = 1 mm. B, Cotyledons and rosette leaves in the order of appearance (from left to right) at 24 d after germination. Bar = 1 cm. C, Fresh weight of rosette leaves at 32 d after germination. D, Average size of abaxial epidermal cells of the sixth rosette leaf of wild-type (WT) and *rock2* plants ($n = 14$). E, Leaf area of the sixth fully grown rosette leaf. The statistical significance of differences compared with the wild type was calculated by ANOVA. *, $P < 0.001$.

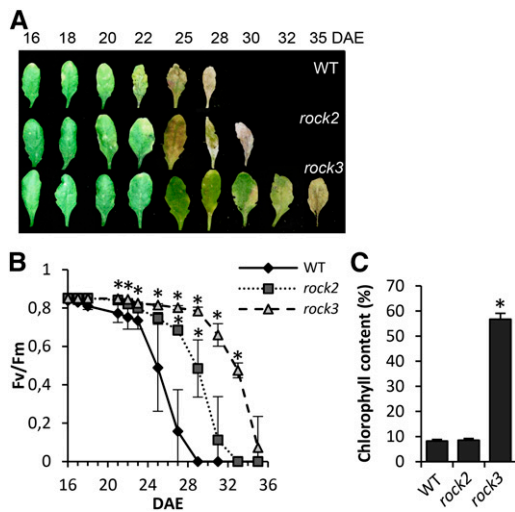


Figure 7. Natural and dark-induced leaf senescence. A, Age-dependent senescence phenotypes of the sixth leaf of the wild type (WT) and *rock2/rock3* mutants grown under long-day conditions starting at 16 d after leaf emergence (DAE). B, F_v/F_m of the sixth leaf at the time points shown in A. C, Dark-induced senescence in a detached leaf assay. The chlorophyll content of the sixth leaf was examined after 7 d in the dark. The leaf chlorophyll content before the start of dark incubation was set at 100% for each genotype tested ($n = 10$). Error bars represent sd. The statistical significance of differences compared with the wild type was calculated by ANOVA. *, $P < 0.001$.

***rock2* and *rock3* Alter Flowering Time and Increase Flower Size and Seed Yield**

Under long-day conditions, *rock2* mutants and *AHK2:rock2* transgenic lines flowered significantly earlier than the wild type, as indicated by their lower number of rosette leaves at flowering time (Fig. 8A). Likewise, the *AHK3:rock3* transgenic plants, but not the *rock3* mutant, flowered earlier. Interestingly, all mutant and transgenic lines also showed a markedly increased duration of flowering and increased total life span. Seven-week-old wild-type plants ceased to form new flowers, while *rock* genotypes continued to flower for at least 1 week and up to 2 weeks in the case of *AHK2:rock2* transgenic plants (Fig. 8B).

The size of flowers was enhanced significantly in *rock2* and *rock3* mutants (Fig. 8C). To determine whether the increase in petal size was the result of increased cell proliferation, cell expansion, or both, abaxial petal epidermal cell size was analyzed exemplarily in *AHK2:rock2* flowers. Figure 8D shows that the cell size was not altered significantly, indicating that an enhanced cell proliferation was the cause for the larger petals, similar to that found for rosette leaf size regulation (Fig. 6, D and E).

rock2, *AHK2:rock2*, and *AHK3:rock3* plants formed more siliques than wild-type plants (Fig. 8E). The transgenic *AHK2:rock2* line showed the largest increase, producing almost twice as many siliques as the wild type. Interestingly, despite the activity of cytokinin in regulating shoot meristem activity and size (Bartrina et al., 2011), microscopic analysis did not reveal an

increased size of *rock2* or *rock3* inflorescence meristems (Supplemental Fig. S3). Consistently, the analysis of cytokinin signaling output in the inflorescence meristem of *rock2* plants using the *TCSn:GFP* marker gene (Zürcher et al., 2013) showed no significant change in comparison with the wild type (Supplemental Fig. S3), suggesting a dampening of the increased receptor signaling in the inflorescence meristem. This indicates that the formation of more flowers and, consequently, of more siliques was due to a longer flowering phase. Analysis of seed yield did not show an increase in plants harboring a

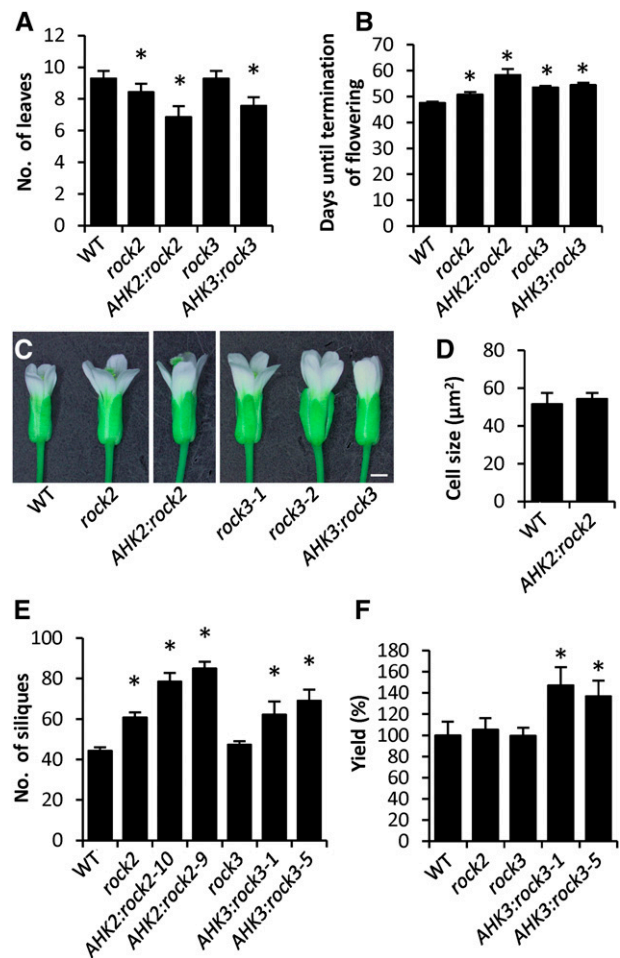


Figure 8. *rock2* and *rock3* positively regulate flowering time and flower size. A, Number of rosette leaves at the start of flowering of plants grown under long-day conditions. B, *rock2* and *rock3* mutants and transgenic plants flower longer than the wild type (WT). Shown are days until the termination of flowering ($n = 10$). C, Flowers of *rock2* and *rock3* mutants and transgenic lines compared with the wild type. Bar length is 500 μm . D, Average size of abaxial epidermal cells of petals at stage 13 (Smyth et al., 1990; $n = 5$). E, Number of siliques on the main stem. Siliques, including unfilled and partially filled siliques, were counted after the end of flowering ($n = 15$). F, Seed yield of *rock2* and *rock3* mutants and transgenic lines compared with the wild type. The seed yield of the wild type was set to 100%. Error bars represent sd. The statistical significance of differences compared with the wild type was calculated by Student's *t* test. *, $P < 0.005$.

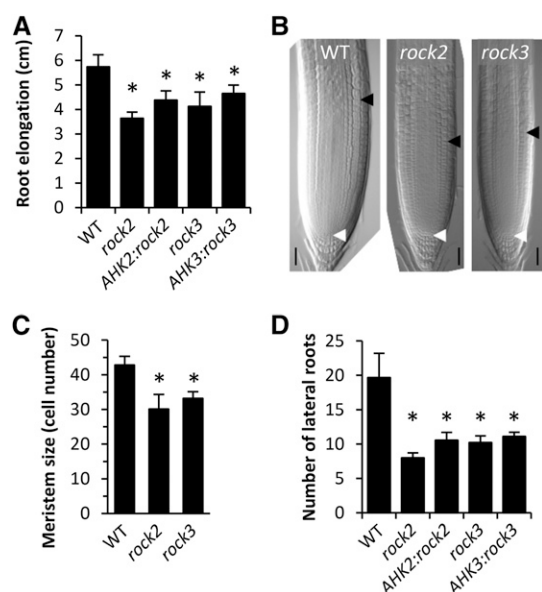


Figure 9. The *rock2* and *rock3* mutants have reduced root systems. *A*, Elongation of primary roots between day 4 and day 12 after germination ($n = 20$). *B*, Root meristems of the wild type (WT), *rock2*, and *rock3*. Roots were analyzed 5 d after germination. White and black arrowheads indicate, respectively, the quiescent center and the start of the transition zone. Bars = 50 μm . *C*, Number of cortex cells between the quiescent center and the start of the transition zone ($n = 10$). *D*, Number of lateral roots at 12 d after germination ($n = 20$). Error bars represent sd. The statistical significance of differences compared with the wild type was calculated by Student's *t* test. *, $P < 0.005$.

rock2 allele, which was probably accountable to heterostylous flowers displaying disproportionately elongated gynoecia in comparison with the stamen, which caused reduced self-fertilization (Supplemental Fig. S4). However, *AHK3:rock3* plants lacking this morphological defect produced about 40% more seeds than wild-type plants. A similar result was found for a second transgenic *rock3* line (*AHK3:rock3-5*), confirming that seed yield is positively influenced by the *rock3* mutation.

rock2 and *rock3* Reduce Root Growth

In contrast to its promotional role in shoot organs, cytokinin is a negative regulator of root development (Werner and Schmülling, 2009). As expected from the observed suppressor activity (Fig. 1H), root growth was inhibited in all tested *rock* seedlings grown under in vitro conditions (Fig. 9A). Primary root elongation was reduced by 37% and 28% in *rock2* and *rock3* seedlings, respectively. The transgenic *rock* lines *AHK2:rock2-10* and *AHK3:rock3-1* showed slightly milder root phenotypes, with reductions in root elongation of 23% and 18%, respectively (Fig. 9A). Consistently, root meristem size was decreased in both the *rock2* and *rock3* mutants (Fig. 9, B and C). The formation of lateral roots was strongly inhibited as well. On average, the number of lateral roots in wild-type plants was around 1.8 to 2.4

times greater than that of the *rock* mutants, with *rock2* showing the strongest reduction of lateral root formation (Fig. 9D). The similar or even weaker consequences of transgenic *rock* gene expression compared with their original alleles contrasts with their generally stronger effects on the shoot phenotype.

DISCUSSION

From the analysis of the *rock2* and *rock3* mutant alleles and transgenic lines carrying these alleles, we obtained valuable information about the cytokinin signaling mechanism and the roles of these redundantly acting receptors in regulating various facets of the plant's phenotype. Both aspects are discussed in the following sections.

rock2 and *rock3* Mutations Provide Insight into Transmembrane Signaling by Cytokinin Receptors

How the cytokinin signal is transmitted across the membrane is an entirely unknown process. The *rock2* and *rock3* mutations identified several amino acid

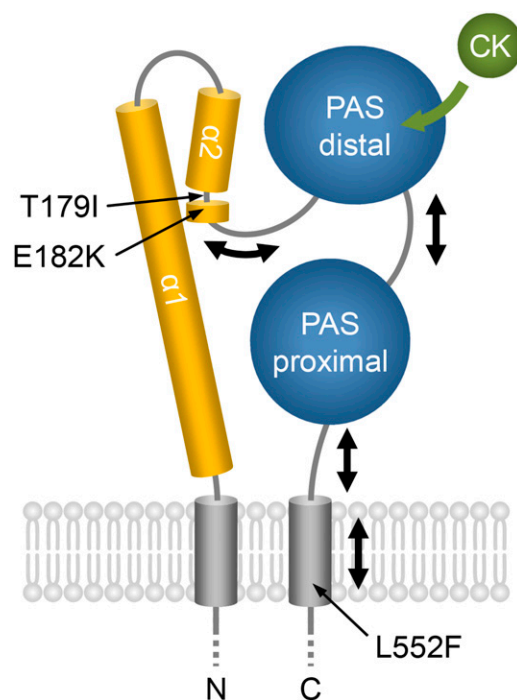


Figure 10. Model of conformational changes associated with transmembrane signaling following cytokinin perception. The schematic topology of the sensory module of cytokinin receptors is based on the crystal structure of AHK4 (Hothorn et al., 2011). The N-terminal helices ($\alpha 1$, $\alpha 2$, and its neighboring 3_{10} -helix) of the CHASE domain are shown in orange, and the two PAS domains are depicted schematically. The model predicts that cytokinin binding causes reversible conformational changes (double-headed arrows), causing a piston-type displacement of the different subdomains and ultimately resulting in the transmission of the signal across the membrane. *rock2* and *rock3* mutations (arrows) are predicted to mimic those changes locking the receptor in a constitutively active conformation.

residues that are relevant for transmembrane signaling. Presumably, they induce changes in the receptor structure resembling those induced by cytokinin binding to the CHASE domain and, thus, cause constitutive cytokinin signaling. The fact that the AHK4 receptors harboring *rock2* and *rock3* mutations conferred growth rescue of $\Delta sln1$ yeast to a great extent similar to that caused by cytokinin-induced signaling of wild-type AHK4 suggests that these mutations cause strong, if not maximal, activation of the receptors.

We isolated two independent *rock3* mutations that are located in close proximity to each other in a region of the CHASE domain linking the long α -helical stalk domain with the membrane-distal (ligand-binding) PAS domain (Hothorn et al., 2011). More precisely, they are located in a slightly bent region comprising a 3_{10} -helix that connects helix $\alpha 2$ with the first β -strand of the membrane-distal PAS domain (Hothorn et al., 2011; Fig. 10). This region, which is not involved in ligand binding, could participate in the receptor domain movement expected to be triggered by cytokinin binding. The *rock3* mutations, which alter evolutionarily highly conserved residues (Heyl et al., 2007; Steklov et al., 2013), may provoke a similar intramolecular movement.

There is an intriguing structural similarity between the CHASE domain and the sensing domain of a bacterial methyl-accepting chemotaxis protein (MCP), which is a membrane-bound His kinase recognizing Ile. The sensory domains of both receptor types have a long α -helical stalk important to keep the receptor dimers together and to hold two PAS domains, of which the membrane-distal one binds the ligand (Hothorn et al., 2011; Liu et al., 2015). Analysis of the ligand-induced conformational changes of the PAS-sensing domain of MCP revealed that it likely signals by a piston-displacement mechanism (Liu et al., 2015). The signal-binding PAS domain fluctuates between a closed (ligand-bound) and open form, resulting in a conformational change of the proximal PAS domain and movement toward and away from the membrane. This movement is propagated, causing a displacement of the transmembrane helix toward the cytoplasm, thus generating a transmembrane signal (Liu et al., 2015). Considering the close structural similarity between cytokinin receptors and MCP as well as the fact that piston-type signaling is a common theme among other types of His kinases (Chervitz and Falke, 1996; Cheung and Hendrickson, 2009; Moore and Hendrickson, 2009; Bhate et al., 2015), we hypothesize that the CHASE domain also undergoes, upon ligand binding, structural changes emulating a piston-like domain motion resulting in transmembrane signaling (Fig. 10). Interestingly, the last β -strand of the membrane-proximal PAS domain is linked to the stalk helix by a disulfide bridge (Hothorn et al., 2011), which might limit the degree of structural rearrangements. Hence, the domain displacement will probably be of a subtle nature, as known for other His kinases (Chervitz and Falke, 1996).

The *rock2* mutation is located in the transmembrane domain connecting the CHASE domain and the

cytosolic His kinase domain. In the proposed signaling mechanism (Fig. 10), this transmembrane domain is essential for transmitting the signal from the lumen of the endoplasmic reticulum to the cytoplasm. Noteworthy, this transmembrane domain shows a high degree of sequence conservation among different cytokinin receptors, in contrast to the transmembrane domain delimiting the CHASE domain N terminally (Steklov et al., 2013). The L552F substitution in the *rock2* receptor variant affects the highly conserved Leu residue of the helix core motif Axxx(S/A)x(G/L)x(L/F)Vix(L/F)LxG(Y/H)I (Leu-552 underlined). Furthermore, this residue is located in the immediate vicinity of two gain-of-function mutations of the AHK4 receptor that have been reported to cause constitutive cytokinin signaling in a bacterial assay (Miwa et al., 2007) and that are partially conserved in AHK2. Presumably, the described mutations cause constitutive conformational alterations of the transmembrane domain, which normally occur during signaling. Although no crystal structure for any transmembrane domain of any His kinase has been resolved to date, there is a growing body of knowledge (Bhate et al., 2015) allowing us to predict that the structural changes may involve a lateral or vertical displacement of the neighboring transmembrane helices and that such a displaced conformation is being locked by the *rock2* and related mutations.

Constitutively Active Receptors Yield Novel Information About Cytokinin-Regulated Processes

The analysis of mutants and transgenic lines expressing constitutively active variants of two cytokinin receptors has revealed how plants with locally strongly enhanced cytokinin signaling look. Only a single gain-of-function cytokinin receptor mutant, *ore12*, has been described previously in Arabidopsis (Kim et al., 2006), but the description has been limited to the impact on leaf senescence. In addition, the *ore12* mutation achieved a lower activation of the AHK3 receptor compared with the *rock3* mutations described here, suggesting that this receptor signals in a gradual rather than an all-or-nothing fashion. Others reported that the production of transgenic plants expressing constitutively active receptors was difficult if not impossible (Miwa et al., 2007). Studying the influence of enhanced cytokinin signaling on the plant phenotype is relevant as, until now, our knowledge of the consequences of an enhanced cytokinin status has been derived largely from plants ectopically expressing a cytokinin-synthesizing *ISOPENTENYLTRANSFERASE* (Rupp et al., 1999; Sun et al., 2003) or *LONELY GUY* (Kuroha et al., 2009) gene or carrying mutations in cytokinin-degrading *CKX* genes (Bartrina et al., 2011). However, the impact of an enhanced production of the hormone may differ from the consequences of increased signaling. The former involves a mobile signal that can induce local but also systemic effects through all cytokinin receptors

that are present in a given cell or tissue, while the latter acts in a cell-autonomous fashion involving only a single activated receptor. In accord with this notion, the expression of the *ARR5:GUS* gene confirmed enhanced cytokinin signaling by *rock2* and *rock3* and showed that signaling generally stays limited to those tissues known previously to activate the cytokinin reporter by the corresponding wild-type receptor (D'Agostino et al., 2000; Stolz et al., 2011). Interestingly, *rock2* and *rock3* mutants have reduced levels of all analyzed cytokinin metabolites. This is in agreement with the result that *ahk* loss-of-function mutants have increased cytokinin contents (Riefler et al., 2006) and, thus, underpins the existence of homeostatic control mechanisms. Part of these control mechanisms is an influence of cytokinin signaling on the transcript level of cytokinin metabolism genes (Miyawaki et al., 2004; Werner et al., 2006; Brenner et al., 2012).

Both *rock2* and *rock3* mutations affect most morphological aspects of the cytokinin deficiency syndrome but revert them to a different degree. The similar although not identical effects of these mutations on the plant phenotype reflect their high degree of functional redundancy revealed by loss-of-function mutants (Higuchi et al., 2004; Nishimura et al., 2004; Riefler et al., 2006). There are a number of notable quantitative differences between the *rock2* and *rock3* effects, which also are seen in the differential activation of the *ARR5:GUS* reporter in different tissues. For example, the *rock2* mutation has a stronger impact on primary root elongation and root meristem size, which is surprising in view of the proposed central role that AHK3 (but not AHK2) plays in the root apical meristem (Dello Ioio et al., 2007). Similarly, the late-flowering phenotype of *CKX1ox* plants was only partially reverted by *rock3*, whereas *rock2 CKX1ox* flowered even earlier than the wild type. In contrast, *rock3*, for example, had a stronger effect in retarding leaf senescence. These mostly gradual differences may partly be due to differences in signaling strength caused by the mutations but also may reflect differences in coupling to downstream signaling processes. Indeed, ectopic expression of the *rock2* and *rock3* alleles under the transcriptional control of the same promoters in *Arabidopsis* causes partly different responses (A. Stolz and T. Schmülling, unpublished data). This indicates that, although the cytoplasmic domains of both receptors interact with the same AHP proteins in a yeast two-hybrid assay (Dortay et al., 2006), the affinities between signaling proteins may differ in planta. Their interaction also can be modulated by accessory proteins in a similar fashion to that known from bacterial two-component systems (Jung et al., 2012).

One important result derived from the phenotypic analysis is that cytokinin signaling is limiting for the growth of different shoot organs and that *rock2/rock3*-dependent changes in organ size are due to prolonged cell proliferation. This supports the hypothesis that cytokinin primarily controls the duration of the cell proliferation phase in shoot organ primordia by delaying the onset of cell differentiation (Holst et al.,

2011). Consistently, a lower cytokinin activity causes a reduced leaf size, and genetic analysis has revealed that this is redundantly controlled by AHK2 and AHK3 (Werner et al., 2003; Higuchi et al., 2004; Nishimura et al., 2004; Riefler et al., 2006). It has been proposed that plant organ growth displays bell-shaped dose responses to cytokinin (Ferreira and Kieber, 2005) and that cytokinin limits leaf size in the wild type (Efroni et al., 2013). The enhanced growth of different shoot organs in *rock2* and *rock3* mutants underpins this view. However, the range of cytokinin activity promoting growth appears to be limited, since cytokinin overproduction may result in the formation of smaller leaves (Hewelt et al., 1994; van der Graaff et al., 2001; Sun et al., 2003). This is likely due to strongly increased cell proliferation and the concomitant inability of proper cell differentiation and expansion. Cell number is apparently sensed in plant leaves (Hisanaga et al., 2015), and an increase in cell number above a certain threshold may interfere with cell expansion, resulting in smaller leaves (Dewitte et al., 2003). The increased cell proliferation in *rock2* and *rock3* mutants was linked to normal cell expansion, suggesting that this threshold was not reached. Our work here further revealed that flower organ size is very sensitive to enhanced cytokinin signaling too. The particularly strongly enlarged petals and gynoecia suggest that cytokinin is especially involved in regulating the development of these organs.

For a long time, it has been known that exogenously applied cytokinin can promote flowering in *Arabidopsis* (Michniewicz and Kamienska, 1967; Besnard-Wibaut, 1981; Dennis et al., 1996; D'Aloia et al., 2011). However, it has remained unclear whether endogenous cytokinin also would have the same promotive activity. *rock2* suppresses the late-flowering phenotype of *CKX1ox* plants more strongly than *rock3*. This effect is most obvious under short-day conditions, where *CKX1ox* remains in the vegetative state and *rock2*, but not *rock3*, reverts this nonflowering phenotype. It seems clear that, in *Arabidopsis*, a certain cytokinin threshold signal is indispensable for flower induction in short days and that cytokinin has a promotive effect on flowering also in long days. The fact that *rock2 CKX1ox* mutants start to flower even earlier than the wild type underpins the importance of cytokinin signaling for flowering time control. The mechanistic basis of flowering time control by cytokinin is poorly understood. It has been shown that cytokinin promotes flowering independently of *FLOWERING LOCUS T* but through the transcriptional activation of its paralogue *TWIN SISTER OF FLOWERING LOCUS T (TSF)*; D'Aloia et al., 2011). However, the question of whether the flowering response to cytokinin is mediated entirely through the transcriptional activation of *TSF* in leaves or whether cytokinin also might promote flowering by direct action in the shoot apical meristem (Corbesier et al., 2003; D'Aloia et al., 2011) needs to be scrutinized further.

An unexpected phenotype was the increased plant longevity and prolonged reproductive growth phase,

which was particularly marked in transgenic plants. The prolonged reproductive growth resulted in a strongly increased number of flowers and siliques. This is a very interesting observation, because the monocarpic plant *Arabidopsis* generates dependent on the growth conditions a specific number of flowers, which is followed by the cessation of reproductive meristematic activity. This correlative inhibition of maternal growth is caused by the offspring (seeds) and is referred to as global proliferative arrest (GPA; Hensel et al., 1994). The molecular mechanism underlying this phenomenon is largely unknown. A recent study has suggested that the low mitotic activity in meristems linked to GPA represents a form of bud dormancy (Wuest et al., 2016). Given that cytokinin is a major factor determining the proliferative activity in axillary buds (Shimizu-Sato et al., 2009), it is tempting to hypothesize that cytokinin counteracts GPA by maintaining cell division activity. This scenario would predict that a drop in cytokinin activity is required for meristematic arrest during GPA and that the constitutive signaling in *rock2* and *rock3* transgenic plants delays it. How cytokinin could affect GPA is currently unclear. One possibility is that *rock2* and *rock3*, and thus cytokinin, acts locally in the reproductive meristem by sustaining its activity. This idea is consistent with the previous hypothesis that meristematic sink activity, rather than the leaf source capacity, is decisive for the activity of the meristem and that sink strength is particularly triggered by cytokinin (Werner et al., 2008). A second possibility is that the strong capacity of *rock3* to delay leaf senescence prolongs the activity of the reproductive meristems and, in addition, provides sufficient source capacity to support the development of supernumerary seeds. However, it has also been discussed that the activity of the reproductive meristem is uncoupled from rosette leaf senescence in *Arabidopsis* (Hensel et al., 1993; Noodén and Penney, 2001; Wuest et al., 2016). The two possibilities are not mutually exclusive, and further research is needed to understand the mechanism underlying the action of cytokinin during GPA.

In the above context, it is noteworthy that the size of the inflorescence meristems of *rock2* and *rock3* mutants was not increased, although these receptors are expressed and active in the meristem (Riefler et al., 2006; Stolz et al., 2011; Gruel et al., 2016). This is surprising considering that plants producing more or less cytokinin develop a larger or smaller inflorescence meristem, respectively (Bartrina et al., 2011). One plausible explanation for these apparently incongruous observations might be that, in tissues where *AHK2* and *AHK3* expression overlaps that of *AHK4*, as in the inflorescence meristem (Gruel et al., 2016), the enhanced signaling activity might be dampened by the phosphatase activity of *AHK4* (Mähönen et al., 2006). In the presence of low cytokinin (as in the *rock2* and *rock3* plants), the phosphatase activity of the *AHK4* receptor may prevail and alleviate downstream signaling, thus counteracting the enhanced kinase activity of *rock2* and *rock3* receptors. Consistent with this idea, the

TCSn:GFP cytokinin reporter indicated similar signaling output activity in wild-type and *rock2* inflorescence meristems. In this respect, it would be interesting to analyze the *rock2* and *rock3* mutations in an *ahk4* null mutant background (Inoue et al., 2001). In contrast to *rock2/rock3* plants, the *ckx3 ckx5* mutation (Bartrina et al., 2011) presumably increases the signaling output of all three cytokinin receptors and lowers the phosphatase activity of *AHK4*; together, this might lead to a quantitatively and qualitatively different cytokinin output signal.

Last but not least, transgenic expression of the *rock3-1* allele caused an ~50% higher seed yield, which is similar to that brought about by the *ckx3 ckx5* mutation (Bartrina et al., 2011). However, the mechanisms leading to increased seed yield appear to be at least partly different. *ckx3 ckx5* mutants have a larger inflorescence meristem forming an increased number of flowers and siliques. In addition, siliques contain more seeds due to an increased placenta activity producing more ovules (Bartrina et al., 2011). In the case of *rock3* transgenic plants, enhanced yield was due mainly to delayed GPA (see above), leading to taller plants with more siliques (*rock2* transgenic plants formed even more flowers but suffered from reduced fertilization). In sum, our results corroborate the role of cytokinin as a regulator of seed yield (Ashikari et al., 2005; Bartrina et al., 2011) and demonstrate that different developmental mechanisms can be involved. We propose the *rock2* and *rock3* genes as a novel biotechnological tool to achieve yield enhancement. Because the coupling of the receptors to downstream signaling components is promiscuous, they could be used directly for a gain-of-function approach in crop plants to increase cytokinin signaling in a targeted and cell-autonomous fashion.

MATERIALS AND METHODS

Plant Material and Growth Conditions

The Columbia ecotype of *Arabidopsis* (*Arabidopsis thaliana*) was used as the wild type. The following lines were described previously: 35S:CKX1-11 (Werner et al., 2003), *ahk2-5* (Riefler et al., 2006), *ARR5:GUS* (D'Agostino et al., 2000), and *ore12-1* (Kim et al., 2006). All plants were grown on soil or in vitro on one-half-strength Murashige and Skoog medium under long-day (16 h of light/8 h of darkness) or short-day (8 h of light/16 h of darkness) conditions at 22°C. For root growth assays, seedlings were grown on vertical plates, and the length of the primary root was measured between day 4 and day 12 after germination from digital images using Scion Image software (<http://scion-image.software.informer.com/>). For the cytokinin sensitivity assay, BA dissolved in dimethyl sulfoxide or dimethyl sulfoxide as a solvent control was added to the medium.

Mutagenesis and Gene Mapping

The *rock2* and *rock3* mutants were identified in a screen of an M2 population of 35S:CKX1 plants mutagenized with ethyl methanesulfonate (Niemann et al., 2015). Mapping populations for *rock2* and *rock3* were generated by crossing the *rock2* 35S:CKX1 and *rock3* 35S:CKX1 plants with the Landsberg *erecta* ecotype. F2 progeny resistant to hygromycin (cosegregating with 35S:CKX1) and showing the cytokinin deficiency syndrome were used to map the recessive (wild-type) alleles of *rock2* and *rock3*. By analyzing 535 F2 recombinants, *rock2* was mapped to a 1.45-Mb region (~21.1 cM). To map the *rock3* locus, 927 F2 recombinants were analyzed and a 350-kb interval (~0.4 cM) was identified.

The *rock2* and *rock3* mutations were identified by sequencing candidate genes in these intervals and subsequent complementation of 35S:CKX1 transgenic plants by the mutant alleles of the respective gene.

DNA Cloning

The *rock2* and *rock3* point mutations were introduced into the *AHK2:AHK2* and *AHK3:AHK3* genes (Stolz et al., 2011) using the QuickChange site-directed mutagenesis kit (Stratagene). Both constructs were introduced into *Agrobacterium tumefaciens* strain GV3101, and 35S:CKX1 and wild-type plants were transformed using the floral dip method (Clough and Bent, 1998). Transgenic lines were selected on medium containing 50 mg L⁻¹ kanamycin.

Analysis of Transcript Levels by qPCR

Total RNA was extracted from seedlings with the TRIzol method (Thermo Fisher Scientific). Equal amounts of starting material (1 µg of RNA) were used in a 10-µL SuperScript III Reverse Transcriptase reaction (Thermo Fisher Scientific). First-strand cDNA synthesis was primed with a combination of oligo(dT) primers and random hexamers. Real-time qPCR using FAST SYBR Green I technology was performed on the CFX96 Touch Real-Time PCR Detection System (Bio-Rad). The quantitative PCR temperature program consisted of the following steps: 95°C for 15 min; 40 cycles of 95°C for 15 s, 55°C for 15 s, and 72°C for 15 s; followed by melting curve analysis. The relative transcript abundance of each gene was calculated based on the 2^{-ΔΔC_t} method (Livak and Schmittgen, 2001). *PP2AA2* (*At3g25800*) was used for normalization. Primers used for reference genes and genes of interest are listed in Supplemental Table S3.

Yeast Complementation Assay

The yeast complementation assay was performed as described before (Inoue et al., 2001; Mähönen et al., 2006). The *rock2* and *rock3* mutations were introduced into the *AHK4* gene (named *AHK4^{rock2}* and *AHK4^{rock3}*) of plasmid p423TEF-CRE1 (Mähönen et al., 2006) using the QuickChange site-directed mutagenesis kit. After sequence confirmation, plasmids were introduced into yeast strain (TM182) *Δsln1* (Inoue et al., 2001), and the yeast complementation assay was performed with either 2% Gal or 2% Glc (w/v) with 0.1 or 10 µM tZ added to the medium. Optical density at 600 nm was measured after 20 h.

GUS Staining, Microscopy, and Scanning Electron Microscopy

GUS staining was performed as described by Köllmer et al. (2014). For microscopic analysis, tissues were cleared according to Malamy and Benfey (1997). Hand-cut cross sections of stems from 5-week-old plants were stained for 5 min in 0.02% aqueous Toluidine Blue O, rinsed, and mounted in water. All samples were viewed with an Axioskop 2 plus microscope (Zeiss). The inflorescence meristem of the main stem from 4-week-old soil-grown plants was dissected and analyzed by scanning electron microscopy as described before (Bartrina et al., 2011). TCSn:GFP fluorescence was analyzed according to Zürcher et al. (2013) using a Leica SP5 confocal microscope. Root meristem size was determined as described by Dello Ioio et al. (2007).

Determination of Cytokinin Content

Plants were grown in vitro for 14 d. For each sample, 100 mg of seedlings was pooled, and five independent samples were analyzed for each genotype. The cytokinin content was determined by ultra-performance liquid chromatography-electrospray-tandem mass spectrometry (Novák et al., 2008).

Analysis of Leaf Senescence and Photosynthetic Parameters

For the analysis of dark-induced leaf senescence, seedlings were grown in vitro for 18 d. The sixth rosette leaf was detached and floated on distilled water. After 7 d in the dark at room temperature, chlorophyll was extracted as described before (Köllmer et al., 2011). The *F_v/F_m* ratio of dark-adapted plants was measured with FluorCam (Photon Systems Instruments).

Determination of Flowering Time, Stem Diameter, Plant Height, and Yield Parameters

For flowering time analysis, seeds were stratified for 3 d at 4°C and sown on soil. The onset of flowering was defined as the plant age when the first flower was visible. The termination of flowering was defined as the time point when no new flowers were formed at the main inflorescence. The number of rosette leaves was scored at the onset of flowering. The diameter of the main inflorescence stem was determined when individual stems reached a height of 15 cm. The hand-made transverse sections were taken 1 cm above the rosette. The final plant height and the number of siliques were determined after the termination of flowering. For the analysis of seed yield, the weight of all fully ripened and desiccated seeds was determined.

Petal Surface Area and Cell Size Measurement

The petal surface area was measured from digital images of fully expanded organs with Scion Image. Petals were cleared (Malamy and Benfey, 1997), and average cell sizes were calculated from the number of cells per unit area of digital micrographs.

Accession Numbers

Sequence data from this article can be found in the GenBank/EMBL data libraries under accession numbers *AHK2* (At5G35750), *AHK3* (At1G27320), *AHK4* (At2G01830), *CKX1* (At2G41510), *ARR5* (At3G48100), *PP2AA2* (At3G25800).

Supplemental Data

The following supplemental materials are available.

Supplemental Figure S1. Expression of *AHK2* and *AHK3* in different genotypes.

Supplemental Figure S2. Comparison of leaf senescence in the wild type, *rock2*, *rock3*, and *ore12*.

Supplemental Figure S3. Size and cytokinin activity in inflorescence meristems.

Supplemental Figure S4. Flower size and morphology of *rock2* and *rock3* mutants compared with the wild type.

Supplemental Table S1. Genetic analysis of the *rock2* and *rock3* mutations.

Supplemental Table S2. Cytokinin content of *rock2* *CKX1ox* and *rock3* *CKX1ox*.

Supplemental Table S3. Oligonucleotide primers used in this study.

ACKNOWLEDGMENTS

We thank Ildoo Hwang for seeds of the *ore12* mutant and Bruno Müller for the *TCSn:GFP* line.

Received December 16, 2016; accepted January 9, 2017; published January 17, 2017.

LITERATURE CITED

- Ainley WM, McNeil KJ, Hill JW, Lingle WL, Simpson RB, Brenner ML, Nagao RT, Key JL (1993) Regulatable endogenous production of cytokinins up to 'toxic' levels in transgenic plants and plant tissues. *Plant Mol Biol* 22: 13–23
- Ashikari M, Sakakibara H, Lin S, Yamamoto T, Takashi T, Nishimura A, Angeles ER, Qian Q, Kitano H, Matsuoka M (2005) Cytokinin oxidase regulates rice grain production. *Science* 309: 741–745
- Bartrina I, Otto E, Strnad M, Werner T, Schumlling T (2011) Cytokinin regulates the activity of reproductive meristems, flower organ size, ovule formation, and thus seed yield in *Arabidopsis thaliana*. *Plant Cell* 23: 69–80
- Besnard-Wibaut C (1981) Effectiveness of gibberellins and 6-benzyladenine on flowering of *Arabidopsis thaliana*. *Physiol Plant* 53: 205–212

- Bhargava A, Clabaugh I, To JP, Maxwell BB, Chiang YH, Schaller GE, Loraine A, Kieber JJ (2013) Identification of cytokinin-responsive genes using microarray meta-analysis and RNA-Seq in *Arabidopsis*. *Plant Physiol* **162**: 272–294
- Bhate MP, Molnar KS, Goulian M, DeGrado WF (2015) Signal transduction in histidine kinases: insights from new structures. *Structure* **23**: 981–994
- Brenner WG, Ramireddy E, Heyl A, Schmülling T (2012) Gene regulation by cytokinin in *Arabidopsis*. *Front Plant Sci* **3**: 8
- Brenner WG, Schmülling T (2015) Summarizing and exploring data of a decade of cytokinin-related transcriptomics. *Front Plant Sci* **6**: 29
- Caesar K, Thamm AMK, Witthöft J, Elgass K, Huppenberger P, Grefen C, Horak J, Harter K (2011) Evidence for the localization of the *Arabidopsis* cytokinin receptors AHK3 and AHK4 in the endoplasmic reticulum. *J Exp Bot* **62**: 5571–5580
- Chervitz SA, Falke JJ (1996) Molecular mechanism of transmembrane signaling by the aspartate receptor: a model. *Proc Natl Acad Sci USA* **93**: 2545–2550
- Cheung J, Hendrickson WA (2009) Structural analysis of ligand stimulation of the histidine kinase NarX. *Structure* **17**: 190–201
- Clough SJ, Bent AF (1998) Floral dip: a simplified method for *Agrobacterium*-mediated transformation of *Arabidopsis thaliana*. *Plant J* **16**: 735–743
- Corbesier L, Prinsen E, Jacqumard A, Lejeune P, Van Onckelen H, Périlleux C, Bernier G (2003) Cytokinin levels in leaves, leaf exudate and shoot apical meristem of *Arabidopsis thaliana* during floral transition. *J Exp Bot* **54**: 2511–2517
- Cortleven A, Nitschke S, Klaumünzer M, Abdelgawad H, Asard H, Grimm B, Riefler M, Schmülling T (2014) A novel protective function for cytokinin in the light stress response is mediated by the ARABIDOPSIS HISTIDINE KINASE2 and ARABIDOPSIS HISTIDINE KINASE3 receptors. *Plant Physiol* **164**: 1470–1483
- D'Agostino IB, Deruère J, Kieber JJ (2000) Characterization of the response of the *Arabidopsis* response regulator gene family to cytokinin. *Plant Physiol* **124**: 1706–1717
- D'Aloia M, Bonhomme D, Bouché F, Tamseddak K, Ormenese S, Torti S, Coupland G, Périlleux C (2011) Cytokinin promotes flowering of *Arabidopsis* via transcriptional activation of the FT paralogue TSF. *Plant J* **65**: 972–979
- Dello Iorio R, Linhares FS, Scacchi E, Casamitjana-Martinez E, Heidstra R, Costantino P, Sabatini S (2007) Cytokinins determine *Arabidopsis* root-meristem size by controlling cell differentiation. *Curr Biol* **17**: 678–682
- Dennis ES, Finnegan EJ, Bilodeau P, Chaudhury A, Genger R, Helliwell CA, Sheldon CC, Bagnall DJ, Peacock WJ (1996) Vernalization and the initiation of flowering. *Semin Cell Dev Biol* **7**: 441–448
- Dewitte W, Riou-Khamlichi C, Scofield S, Healy JMS, Jacqumard A, Kilby NJ, Murray JAH (2003) Altered cell cycle distribution, hyperplasia, and inhibited differentiation in *Arabidopsis* caused by the D-type cyclin CYCD3. *Plant Cell* **15**: 79–92
- Dortay H, Mehnert N, Bürkle L, Schmülling T, Heyl A (2006) Analysis of protein interactions within the cytokinin-signaling pathway of *Arabidopsis thaliana*. *FEBS J* **273**: 4631–4644
- Efroni I, Han SK, Kim HJ, Wu MF, Steiner E, Birnbaum KD, Hong JC, Eshed Y, Wagner D (2013) Regulation of leaf maturation by chromatin-mediated modulation of cytokinin responses. *Dev Cell* **24**: 438–445
- Ferreira FJ, Kieber JJ (2005) Cytokinin signaling. *Curr Opin Plant Biol* **8**: 518–525
- Franco-Zorrilla JM, Martín AC, Leyva A, Paz-Ares J (2005) Interaction between phosphate-starvation, sugar, and cytokinin signaling in *Arabidopsis* and the roles of cytokinin receptors CRE1/AHK4 and AHK3. *Plant Physiol* **138**: 847–857
- Gan S, Amasino RM (1995) Inhibition of leaf senescence by autoregulated production of cytokinin. *Science* **270**: 1986–1988
- Gruel J, Landrein B, Tarr P, Schuster C, Refahi Y, Sampathkumar A, Hamant O, Meyerowitz EM, Jönsson H (2016) An epidermis-driven mechanism positions and scales stem cell niches in plants. *Sci Adv* **2**: e1500989
- Hensel LL, Grbić V, Baumgarten DA, Bleecker AB (1993) Developmental and age-related processes that influence the longevity and senescence of photosynthetic tissues in *Arabidopsis*. *Plant Cell* **5**: 553–564
- Hensel LL, Nelson MA, Richmond TA, Bleecker AB (1994) The fate of inflorescence meristems is controlled by developing fruits in *Arabidopsis*. *Plant Physiol* **106**: 863–876
- Hewelt A, Prinsen E, Schell J, Van Onckelen H, Schmülling T (1994) Promoter tagging with a promoterless ipt gene leads to cytokinin-induced phenotypic variability in transgenic tobacco plants: implications of gene dosage effects. *Plant J* **6**: 879–891
- Heyl A, Riefler M, Romanov GA, Schmülling T (2012) Properties, functions and evolution of cytokinin receptors. *Eur J Cell Biol* **91**: 246–256
- Heyl A, Wulfetange K, Pils B, Nielsen N, Romanov GA, Schmülling T (2007) Evolutionary proteomics identifies amino acids essential for ligand-binding of the cytokinin receptor CHASE domain. *BMC Evol Biol* **7**: 62
- Higuchi M, Pischke MS, Mähönen AP, Miyawaki K, Hashimoto Y, Seki M, Kobayashi M, Shinozaki K, Kato T, Tabata S, et al (2004) In planta functions of the *Arabidopsis* cytokinin receptor family. *Proc Natl Acad Sci USA* **101**: 8821–8826
- Hisanaga T, Kawade K, Tsukaya H (2015) Compensation: a key to clarifying the organ-level regulation of lateral organ size in plants. *J Exp Bot* **66**: 1055–1063
- Holst K, Schmülling T, Werner T (2011) Enhanced cytokinin degradation in leaf primordia of transgenic *Arabidopsis* plants reduces leaf size and shoot organ primordia formation. *J Plant Physiol* **168**: 1328–1334
- Hothorn M, Dabi T, Chory J (2011) Structural basis for cytokinin recognition by *Arabidopsis thaliana* histidine kinase 4. *Nat Chem Biol* **7**: 766–768
- Hwang I, Sheen J (2001) Two-component circuitry in *Arabidopsis* cytokinin signal transduction. *Nature* **413**: 383–389
- Inoue T, Higuchi M, Hashimoto Y, Seki M, Kobayashi M, Kato T, Tabata S, Shinozaki K, Kakimoto T (2001) Identification of CRE1 as a cytokinin receptor from *Arabidopsis*. *Nature* **409**: 1060–1063
- Jeon J, Kim NY, Kim S, Kang NY, Novák O, Ku SJ, Cho C, Lee DJ, Lee EJ, Strnad M, et al (2010) A subset of cytokinin two-component signaling system plays a role in cold temperature stress response in *Arabidopsis*. *J Biol Chem* **285**: 23371–23386
- Jung K, Fried L, Behr S, Heermann R (2012) Histidine kinases and response regulators in networks. *Curr Opin Microbiol* **15**: 118–124
- Kieber JJ, Schaller GE (2014) Cytokinins. *The Arabidopsis Book* **12**: e0168, doi/10.1199/tab.0168
- Kim HJ, Ryu H, Hong SH, Woo HR, Lim PO, Lee IC, Sheen J, Nam HG, Hwang I (2006) Cytokinin-mediated control of leaf longevity by AHK3 through phosphorylation of ARR2 in *Arabidopsis*. *Proc Natl Acad Sci USA* **103**: 814–819
- Köllmer I, Novák O, Strnad M, Schmülling T, Werner T (2014) Overexpression of the cytosolic cytokinin oxidase/dehydrogenase (CKX7) from *Arabidopsis* causes specific changes in root growth and xylem differentiation. *Plant J* **78**: 359–371
- Köllmer I, Werner T, Schmülling T (2011) Ectopic expression of different cytokinin-regulated transcription factor genes of *Arabidopsis thaliana* alters plant growth and development. *J Plant Physiol* **168**: 1320–1327
- Kuroha T, Tokunaga H, Kojima M, Ueda N, Ishida T, Nagawa S, Fukuda H, Sugimoto K, Sakakibara H (2009) Functional analyses of LONELY GUY cytokinin-activating enzymes reveal the importance of the direct activation pathway in *Arabidopsis*. *Plant Cell* **21**: 3152–3169
- Liu YC, Machuca MA, Beckham SA, Gunzburg MJ, Roujeinikova A (2015) Structural basis for amino-acid recognition and transmembrane signalling by tandem Per-Arnt-Sim (tandem PAS) chemoreceptor sensory domains. *Acta Crystallogr D Biol Crystallogr* **71**: 2127–2136
- Livak KJ, Schmittgen TD (2001) Analysis of relative gene expression data using real-time quantitative PCR and the $2^{-\Delta\Delta CT}$ method. *Methods* **25**: 402–408
- Lomin SN, Krivosheev DM, Steklov MY, Arkhipov DV, Osolodkin DI, Schmülling T, Romanov GA (2015) Plant membrane assays with cytokinin receptors underpin the unique role of free cytokinin bases as biologically active ligands. *J Exp Bot* **66**: 1851–1863
- Mähönen AP, Bonke M, Kauppinen L, Riikonen M, Benfey PN, Helariutta Y (2000) A novel two-component hybrid molecule regulates vascular morphogenesis of the *Arabidopsis* root. *Genes Dev* **14**: 2938–2943
- Mähönen AP, Higuchi M, Törmäkangas K, Miyawaki K, Pischke MS, Sussman MR, Helariutta Y, Kakimoto T (2006) Cytokinins regulate a bidirectional phosphorelay network in *Arabidopsis*. *Curr Biol* **16**: 1116–1122
- Malamy JE, Benfey PN (1997) Organization and cell differentiation in lateral roots of *Arabidopsis thaliana*. *Development* **124**: 33–44
- Maruyama-Nakashita A, Nakamura Y, Yamaya T, Takahashi H (2004) A novel regulatory pathway of sulfate uptake in *Arabidopsis* roots:

- implication of CRE1/WOL/AHK4-mediated cytokinin-dependent regulation. *Plant J* **38**: 779–789
- Matsumoto-Kitano M, Kusumoto T, Tarkowski P, Kinoshita-Tsujimura K, Václavíková K, Miyawaki K, Kakimoto T** (2008) Cytokinins are central regulators of cambial activity. *Proc Natl Acad Sci USA* **105**: 20027–20031
- Michniewicz M, Kamienska A** (1967) Effect of kinetin on the content of endogenous gibberellins in germinating seeds of some plant species. *Naturwissenschaften* **54**: 372
- Miwa K, Ishikawa K, Terada K, Yamada H, Suzuki T, Yamashino T, Mizuno T** (2007) Identification of amino acid substitutions that render the *Arabidopsis* cytokinin receptor histidine kinase AHK4 constitutively active. *Plant Cell Physiol* **48**: 1809–1814
- Miyawaki K, Matsumoto-Kitano M, Kakimoto T** (2004) Expression of cytokinin biosynthetic isopentenyltransferase genes in *Arabidopsis*: tissue specificity and regulation by auxin, cytokinin, and nitrate. *Plant J* **37**: 128–138
- Moore JO, Hendrickson WA** (2009) Structural analysis of sensor domains from the TMAO-responsive histidine kinase receptor TorS. *Structure* **17**: 1195–1204
- Müller B, Sheen J** (2007) Advances in cytokinin signaling. *Science* **318**: 68–69
- Niemann MCE, Bartrina I, Ashikov A, Weber H, Novák O, Spíchal L, Strnad M, Strasser R, Bakker H, Schmölling T, et al** (2015) *Arabidopsis* ROCK1 transports UDP-GlcNAc/UDP-GalNAc and regulates ER protein quality control and cytokinin activity. *Proc Natl Acad Sci USA* **112**: 291–296
- Nieminen K, Immanen J, Laxell M, Kauppinen L, Tarkowski P, Dolezal K, Tähtiharju S, Elo A, Decourteix M, Ljung K, et al** (2008) Cytokinin signaling regulates cambial development in poplar. *Proc Natl Acad Sci USA* **105**: 20032–20037
- Nishimura C, Ohashi Y, Sato S, Kato T, Tabata S, Ueguchi C** (2004) Histidine kinase homologs that act as cytokinin receptors possess overlapping functions in the regulation of shoot and root growth in *Arabidopsis*. *Plant Cell* **16**: 1365–1377
- Noodén LD, Penney JP** (2001) Correlative controls of senescence and plant death in *Arabidopsis thaliana* (Brassicaceae). *J Exp Bot* **52**: 2151–2159
- Novák O, Hauserová E, Amakorová P, Dolezal K, Strnad M** (2008) Cytokinin profiling in plant tissues using ultra-performance liquid chromatography-electrospray tandem mass spectrometry. *Phytochemistry* **69**: 2214–2224
- Richmond AE, Lang A** (1957) Effect of kinetin on protein content and survival of detached *Xanthium* leaves. *Science* **125**: 650–651
- Riefler M, Novak O, Strnad M, Schmölling T** (2006) *Arabidopsis* cytokinin receptor mutants reveal functions in shoot growth, leaf senescence, seed size, germination, root development, and cytokinin metabolism. *Plant Cell* **18**: 40–54
- Romanov GA, Lomin SN, Schmölling T** (2006) Biochemical characteristics and ligand-binding properties of *Arabidopsis* cytokinin receptor AHK3 compared to CRE1/AHK4 as revealed by a direct binding assay. *J Exp Bot* **57**: 4051–4058
- Rupp HM, Frank M, Werner T, Strnad M, Schmölling T** (1999) Increased steady state mRNA levels of the *STM* and *KNAT1* homeobox genes in cytokinin overproducing *Arabidopsis thaliana* indicate a role for cytokinins in the shoot apical meristem. *Plant J* **18**: 557–563
- Shimizu-Sato S, Tanaka M, Mori H** (2009) Auxin-cytokinin interactions in the control of shoot branching. *Plant Mol Biol* **69**: 429–435
- Smyth DR, Bowman JL, Meyerowitz EM** (1990) Early flower development in *Arabidopsis*. *Plant Cell* **2**: 755–767
- Spíchal L, Rakova NY, Riefler M, Mizuno T, Romanov GA, Strnad M, Schmölling T** (2004) Two cytokinin receptors of *Arabidopsis thaliana*, CRE1/AHK4 and AHK3, differ in their ligand specificity in a bacterial assay. *Plant Cell Physiol* **45**: 1299–1305
- Steklov MY, Lomin SN, Osolodkin DI, Romanov GA** (2013) Structural basis for cytokinin receptor signaling: an evolutionary approach. *Plant Cell Rep* **32**: 781–793
- Stolz A, Riefler M, Lomin SN, Achazi K, Romanov GA, Schmölling T** (2011) The specificity of cytokinin signalling in *Arabidopsis thaliana* is mediated by differing ligand affinities and expression profiles of the receptors. *Plant J* **67**: 157–168
- Sun J, Niu QW, Tarkowski P, Zheng B, Tarkowska D, Sandberg G, Chua NH, Zuo J** (2003) The *Arabidopsis* *AHPT8/PGA22* gene encodes an isopentenyl transferase that is involved in de novo cytokinin biosynthesis. *Plant Physiol* **131**: 167–176
- Suzuki T, Miwa K, Ishikawa K, Yamada H, Aiba H, Mizuno T** (2001) The *Arabidopsis* sensor His-kinase, AHK4, can respond to cytokinins. *Plant Cell Physiol* **42**: 107–113
- Tran LSP, Urao T, Qin F, Maruyama K, Kakimoto T, Shinozaki K, Yamaguchi-Shinozaki K** (2007) Functional analysis of AHK1/ATHK1 and cytokinin receptor histidine kinases in response to abscisic acid, drought, and salt stress in *Arabidopsis*. *Proc Natl Acad Sci USA* **104**: 20623–20628
- Ueguchi C, Sato S, Kato T, Tabata S** (2001) The *AHK4* gene involved in the cytokinin-signaling pathway as a direct receptor molecule in *Arabidopsis thaliana*. *Plant Cell Physiol* **42**: 751–755
- van der Graaff EE, Hooykaas PJJ, Auer CA** (2001) Altered development of *Arabidopsis thaliana* carrying the *Agrobacterium tumefaciens ipt* gene is partially due to ethylene effects. *Plant Growth Regul* **34**: 305–315
- Werner T, Holst K, Pörs Y, Guivarc’h A, Mustroph A, Chriqui D, Grimm B, Schmölling T** (2008) Cytokinin deficiency causes distinct changes of sink and source parameters in tobacco shoots and roots. *J Exp Bot* **59**: 2659–2672
- Werner T, Köllmer I, Bartrina I, Holst K, Schmölling T** (2006) New insights into the biology of cytokinin degradation. *Plant Biol (Stuttg)* **8**: 371–381
- Werner T, Motyka V, Laucou V, Smets R, Van Onckelen H, Schmölling T** (2003) Cytokinin-deficient transgenic *Arabidopsis* plants show multiple developmental alterations indicating opposite functions of cytokinins in the regulation of shoot and root meristem activity. *Plant Cell* **15**: 2532–2550
- Werner T, Schmölling T** (2009) Cytokinin action in plant development. *Curr Opin Plant Biol* **12**: 527–538
- Wuest SE, Philipp MA, Guthörl D, Schmid B, Grossniklaus U** (2016) Seed production affects maternal growth and senescence in *Arabidopsis*. *Plant Physiol* **171**: 392–404
- Wulfetange K, Lomin SN, Romanov GA, Stolz A, Heyl A, Schmölling T** (2011) The cytokinin receptors of *Arabidopsis* are located mainly to the endoplasmic reticulum. *Plant Physiol* **156**: 1808–1818
- Yamada H, Suzuki T, Terada K, Takei K, Ishikawa K, Miwa K, Yamashino T, Mizuno T** (2001) The *Arabidopsis* AHK4 histidine kinase is a cytokinin-binding receptor that transduces cytokinin signals across the membrane. *Plant Cell Physiol* **42**: 1017–1023
- Zürcher E, Müller B** (2016) Cytokinin synthesis, signaling, and function: advances and new insights. *Int Rev Cell Mol Biol* **324**: 1–38
- Zürcher E, Tavor-Deslex D, Litouev D, Enkerli K, Tarr PT, Müller B** (2013) A robust and sensitive synthetic sensor to monitor the transcriptional output of the cytokinin signaling network in planta. *Plant Physiol* **161**: 1066–1075